

Unsupervised Domain Adaptation using Generative Models and Self-ensembling

Eman T. Hassan
Indiana University Bloomington
emhassan@indiana.edu

Xin Chen
Midea ETC
chen1.xin@midea.com

David Crandall
Indiana University Bloomington
djcran@indiana.edu

Abstract

*Transferring knowledge across different datasets is an important approach to successfully train deep models with a small-scale target dataset or when few labeled instances are available. In this paper, we aim at developing a model that can generalize across multiple domain shifts, so that this model can adapt from a single source to multiple targets. This can be achieved by randomizing the generation of the data of various styles to mitigate the domain mismatch. First, we present a new adaptation to the CycleGAN model to produce stochastic style transfer between two image batches of different domains. Second, we enhance the classifier performance by using a self-ensembling technique with a teacher and student model to train on both original and generated data. Finally, we present experimental results on three datasets **Office-31**, **Office-Home**, and **Visual Domain adaptation**. The results suggest that self-ensembling is better than simple data augmentation with the newly generated data and a single model trained this way can have the best performance across all different transfer tasks.*

1. Introduction

Large scale annotated dataset and increasing computational power have enabled the rapid development of deep convolutional networks (CNNs) that produce high performance on many computer vision problems like classification, segmentation, and detection [24, 30, 41]. Unlike human beings who easily generalize knowledge across different domains, it is not easy for CNN models to generalize across other datasets having different characteristics. As a result, domain adaptation, which aims at enhancing the ability of the network to generalize across different domains, has emerged as a hot topic in recent years.

Training a generative model to generate images with different characteristics has witnessed significant progress. Especially after the introduction of Generative Adversarial Networks (GAN) [16]. GANs enable the development of deep models which are capable of image generation

across different domains with high quality [39, 20, 23]. Therefore, GANs have been widely applied to many areas such as image inpainting [36], super-resolution [27], pixel-level domain adaptation [4], and image-to-image translation [54, 18].

That has inspired us to use GANs to randomize the generation of multiple instances of the dataset of different styles to accommodate for any possible unseen domain shifts. We then use these newly generated datasets to effectively enhance knowledge transfer in a teacher-student framework. Previous work [22, 5] has examined using generative networks as a part of the overall adaptation between two domains, while in our case we examine the possibility of generative networks to generate many random instances of the original datasets, where each instance can represent a specific domain shift. Finally we employ the newly obtained datasets to enhance zero-shot domain adaptation.

In this paper, we propose a model that can generalize across different domain shifts. This is accomplished in two steps, the overall proposed system is shown in Figure 1.. First, we introduce stochastic style transfer as an adaptation to the CycleGAN network [54]. It transforms the function of the module from performing one-to-one image translation, to instead perform stochastic style transfer, which generates images with adapted style between the source and target domains. The adaptation depends on relaxing some of the mapping constraints between the two domains. It only checks the mapping between the two domains based on a disentangled representation of the images into style and content representations. Second, we use the trained modules to generate newly adapted datasets. Then, to achieve zero-shot domain adaptation, we develop self-ensembling based domain adaptation, which adapts the teacher-student architecture proposed in [8], where different instances of the same data are the source of perturbation. The experimental results suggest that the newly proposed architecture produces better performance on transferring between one domain to many others.

In summary, we make the following major contributions in this paper:

1. Showing that GAN networks can help make a model

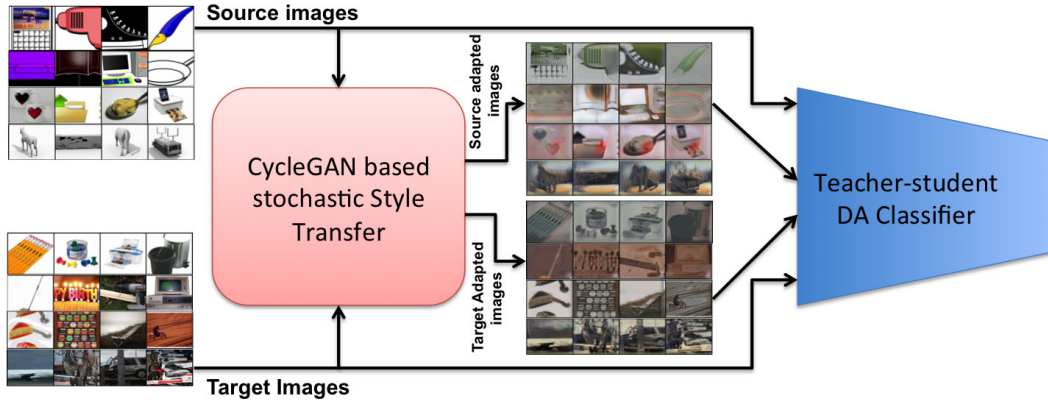


Figure 1: The overall system architecture. The input source and target images are sampled randomly from **Office-31** [43], **Office-Home** [50], and **Visual Domain adaptation** [38] datasets. The images are fed to the CycleGAN-based Stochastic Style Transfer module (explained in more detail in Figure 2). Then style adapted images are generated for both source and target domains. All the images, source and target (both original and adapted), are fed to a teacher-student DA classifier system (explained in more detail in Figure 3).

generalize across multiple domain shifts simultaneously.

2. Using CycleGAN-based architecture to perform stochastic style transfer between the two domains, which helps generate multiple instances of the original datasets.
3. Employing a self-ensembling technique to train a model both in supervised and unsupervised ways using the original datasets and the newly generated instances for both source and target images.
4. Showing that the self-ensembling architecture is better in training than fine tuning with the newly generated data.

2. Related Work

Domain adaptation is a machine learning problem whose goal is that a model trained on a source data $D_s(I_s, Y_s)$ can generalize to related but different data $D_t(I_t, Y_t)$. The source data is fully labeled while the target data is either partially labeled (semi-supervised case) or totally unlabeled (unsupervised case). With this paradigm, many both shallow and deep techniques were proposed to tackle this problem. There are examples of **Shallow Techniques** like Sup-space alignment [9], second order statistic alignment known as CORAL [45], the employment of landmarks to enhance feature alignment [1, 15, 3], sample reweighting [19], and Metric based learning as in [53, 7, 25]. Some examples of **Deep domain adaptation** are knowledge distillation with soft-targets [17] and selectively choosing data samples for fine-tuning [12]. Generally, deep techniques can be categorized into discrepancy based meth-

ods, reconstruction based techniques and adversarial based techniques [6].

Discrepancy based methods as in [31, 32, 51, 46] aim at alignment the deep feature embedding between the source and target domains by optimizing a loss function that penalizes distribution mismatch. Long *et al.* [31] proposed a domain adaptation network that uses a maximum mean discrepancy loss function to match the distribution of the fully connected layers of the source and target networks, while Long *et al.* [32] extended this work by using a joint maximum mean discrepancy loss function instead, and Yan *et al.* [51] incorporated the class weights in the loss function by employing an expectation maximization training paradigm. Similar to CORAL [45] in shallow techniques, Sun *et al.* [46] used Deep CORAL to match the second order statistics between the deep features of the two networks.

Adversarial based techniques [10, 29, 49, 4] use adversarial settings to make the deep feature embeddings of both domains similar. Ganin *et al.* [10] introduced gradient reverse units that reverse the gradient of the domain classifier so that the network learns similar feature representations for both domains. Tzeng *et al.* [48] incorporated loss functions like domain confusion and domain classification in the network framework. Tzeng *et al.* [49] proposed a general framework for unsupervised domain adaptation in both cases of generative or discriminative mappings. Bousmalis *et al.* [4] introduced a technique that adapts source-domain images to appear as if drawn from the target domain. **Reconstruction based techniques** outline how to construct a latent representation that is shared across multiple domains. Ghifary *et al.* [13] considered inter-domain variances as sources of noise in a denoising encoder, then make it learn common features across these different domains. Similarly Ghifary *et al.* [14] proposed a deep reconstruction network

that learns both labeled image prediction and the reconstruction of both target and source images. Bousmalis *et al.* [5] proposed a separation network that learns to separate the latent space into two components, one private to each domain and the other common across different domains. Peng *et al.* [37] proposed a deep generative alignment network that reconstruct images from the source domain that are similar to the target domain and trains the classifier based on these generated images. In our work, we assume a zero-shot framework where we penalize the difference on prediction of the target data, without actually trying to match the distribution of the source domain.

Image-to-Image Translation techniques describe the generation of an image that represents a translation of the input image from one domain to another [21, 54, 18, 55, 22, 35, 28]. Liu *et al.* [28] proposed a UNIT framework for image translation that is based on generative adversarial networks and variational autoencoders that creates a shared latent space which can generate corresponding images between the two domains. Zhu *et al.* [54] presented the CycleGAN model which introduced cycle consistency loss to construct a mapping between the two domains, but this model constructs a one-to-one mapping between the two domain. This work was followed by many papers that introduces models that make the translation many-to-many, as in [55] where Zhu *et al.* introduced a hybrid model that combines conditional variational autoencoder-GANs and Conditional Latent Regressor-GANs. Kang *et al.* [22] used an image generation model to enhance domain adaptation and made the source network guide the attention alignment of the target network in an expectation maximization framework. In our work we extended CycleGAN to generate multiple style adaptations to the original domain to help in knowledge transfer.

Semi-supervised learning and domain adaptation using teacher student model. Zagoruyko *et al.* [52] showed that the performance of a student network is enhanced when it mimics the attention mechanism of the teacher network. Kang *et al.* [22] has employed deep adversarial attention between the two networks to achieve knowledge transfer between the two domains. Mean-teacher model [47] and self-ensembling [26] were proposed in the framework of semi-supervised learning. Laine *et al.* [26] employed the consensus in prediction of the network in training to enhance network performance. While Tarvainen *et al.* [47] proposed the mean teacher model to aggregate information after each step not epoch, in this model the teacher weights used exponential moving average weights of the student model. French *et al.* [8] extended these ideas to the problem of domain adaptation. Meanwhile Luo *et al.* [33] consider the connection between different data points to build a graph that employs a self-ensemble based on smooth neighbors on teacher graphs.

3. Algorithm

3.1. CycleGAN based stochastic Style Transfer

The motivation of this adaptation is how to generate images that have the same contents of the source domain but randomized style that can match in some aspect different domain shifts. The CycleGAN module [54] constructs a mapping between the two domains X, Y as $F : X \rightarrow Y, G : Y \rightarrow X$ where the cycle consistency aims at producing $X \simeq G(F(X))$. That module is designed to produce a one-to-one mapping between the two domains X, Y . We propose a modification to the architecture so that the image generated does not belong to either X or Y , but contains a shared style representation across the two domains. This architecture is shown in Figure 2. The architecture assumes we can obtain a disentangled representation for the images into both content and style representations, so that each domain generator can produce an image that matches the content representation of the original domain and matches random style representation of the other domain. In this way we can benefit from the module to generate multiple random dataset instances that represent different shifts with respect to the original domain.

To get a disentangled feature representation for image I into content I_c and style I_l representation, we employ the method in [11]. An input image I_s is passed through a pre-trained Vgg-16 model [44] where $I_s = \text{relu}_{52}(I)$ and I_t is the concatenation of $Gm(\text{relu}_{12}(I)), Gm(\text{relu}_{22}(I)), Gm(\text{relu}_{33}(I)), Gm(\text{relu}_{43}(I)),$ and $Gm(\text{relu}_{53}(I))$, where Gm represents the gram matrix of the features of $\text{relu}_{ij}(I)$ represents the Rectified Linear Unit activation applied to the output of the j^{th} convolution module in layer i .

In the proposed architecture U_s and U_t represent the source and target generator networks respectively which are implemented using the Unet model architecture [42]. Input images I_s and I_t from the source and target domains are forwarded to the system such that $I_{su} = U_s(I_s)$ and $I_{tu} = U_t(I_t)$. Then the content and style representations are extracted for both input and generated images. For example I_{sc} and I_{sl} are the content and style representations, respectively, of I_s , and similarly I_{tuc} and I_{tul} are the representations for I_{tu} . We introduce an Intra-domain loss function l_{in} and cross domain loss function l_{cross} to be able to generate images with similar contents of the original domain but similar style of the other domain. The Intra-domain loss function l_{in} penalizes the difference in the content representation between the input and generated image of the same domain:

$$L_{in} = MSE(I_{sc}, I_{suc}) + MSE(I_{tc}, I_{tuc}) \quad (1)$$

while the cross domain loss function l_{cross} penalizes the difference in the style representation across the other do-

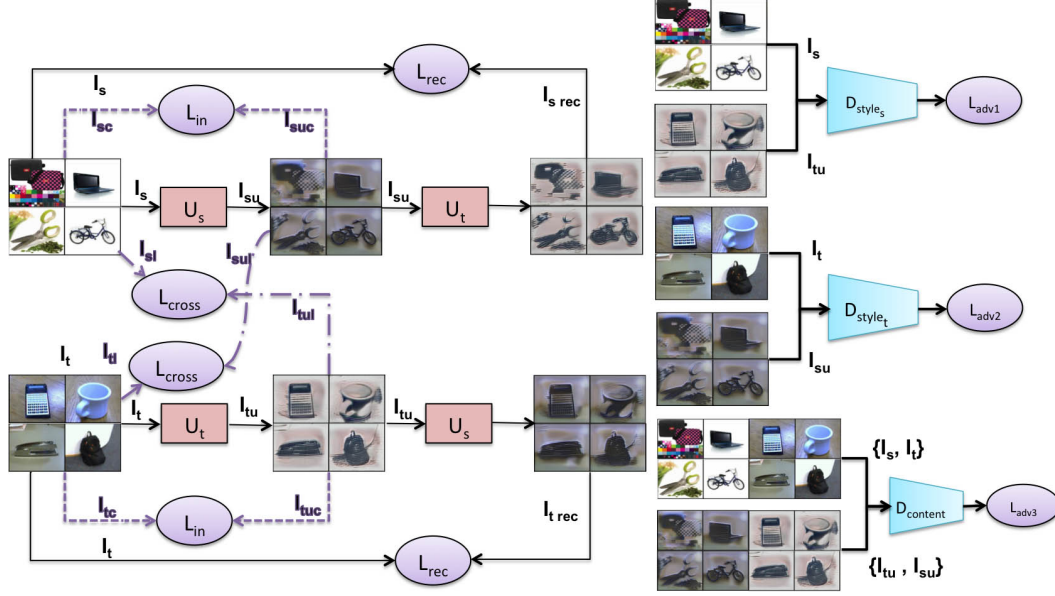


Figure 2: The CycleGAN-based Stochastic Style Transfer module, where input source and target images (sampled randomly from the **Office-31** dataset [43]) are fed to source U_s and target U_t Unets respectively. U_s and U_t nets produce images that match the content of the same domain and the style of the other domain. The resulting images are fed again but to cross domain Unets U_t and U_s respectively to get images that should be similar to the original input images in both content and style. Finally the discriminator networks D_{style_s} and D_{style_t} aim to confuse the generator regarding the style of the source and target domain respectively, while the discriminator network $D_{content}$ aims at fooling the generators to generate realistic images.

main:

$$L_{cross} = MSE(I_{sl}, I_{tul}) + MSE(I_{tl}, I_{sul}) \quad (2)$$

Then we have the cycle loss represented by l_{recons} . The reconstruction loss l_{recons} contributes to training convergence and generating realistic images, and is computed by

$$L_{rec} = MSE(I_s, I_{srec}) + MSE(I_t, I_{trec})$$

where, $I_{srec} = U_t(U_s(I_s))$ (3)

where, $I_{trec} = U_s(U_t(I_t))$

Finally we calculate the adversarial loss functions l_{adv1} , l_{adv2} and l_{adv3} , respectively. Adversarial losses l_{adv1} , l_{adv2} are employed so that the discriminator networks D_{style_s} , D_{style_t} confuse the domain generator networks U_s and U_t to generate images with style similar to the style of the other domain.

$$l_{adv1} = \min_{\{U_s, U_t\}} \max_{D_{style_s}} \{E_{I_s}[\log(D_{style_s}(I_s))] + E_{I_t}[\log(1 - D_{style_s}(U_t(I_t)))]\} \quad (4)$$

$$l_{adv2} = \min_{\{U_s, U_t\}} \max_{D_{style_t}} \{E_{I_t}[\log(D_{style_t}(I_t))] + E_{I_s}[\log(1 - D_{style_t}(U_s(I_s)))]\} \quad (5)$$

On the other hand l_{adv3} and $D_{content}$ confuse the generator networks U_s and U_t to generate realistic images.

$$l_{adv3} = \min_{\{U_s, U_t\}} \max_{D_{content}} \{E_{\{I_s, I_t\}}[\log(D_{content}(\{I_s, I_t\}))] + E_{\{I_s, I_t\}}[1 - \log(D_{content}(\{U_s(I_s), U_t(I_t)\}))]\} \quad (6)$$

The final loss function is a weighted average of these losses, and is computed as:

$$l_{total} = \lambda_1 \times l_{in} + \lambda_2 \times l_{cross} + \lambda_3 \times l_{rec} + \lambda_4 \times l_{adv1} + \lambda_5 \times l_{adv2} + \lambda_6 \times l_{adv3} \quad (7)$$

3.2. Self-ensemble zero shot domain adaptation

The motivation of this section is that simple data augmentation may not be the best way to train a classifier benefiting from the generated images. As shown in Figure 1 that we have both labelled source images and labelled randomly adapted source images and unlabelled target images and unlabelled randomly adapted target images, and data augmentation doesn't explore the dependencies that exists between each image and the corresponding adapted instance.

The idea of a network to have consistent behaviour under different perturbations has been used to enhance the performance of the trained networks [2, 40, 34]. In our work we

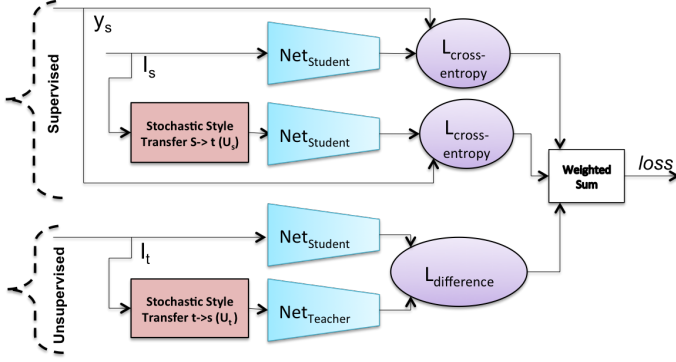


Figure 3: The structure of the ‘Teacher-student’ DA classifier mentioned in Figure 1.

explore the idea that the perturbation can be adding a random new style to the image as shown in Figure 3. In this architecture we extend the framework provided by [8] but we employ the perturbation to be stochastic style transfer between the two domains instead of random data augmentation.

In this model the student is trained in a supervised way using the source dataset instances (the original one $Data_s$ and the style mapped one $Data_{s_m}$). The student model is also trained in an unsupervised manner which is related to the difference in prediction between the student network and the teacher network to the original target data $Data_t$ and style mapped target $Data_{t_m}$. On the other hand, the teacher network model is updated in an exponential moving average manner with the student network. The supervised loss is described by:

$$L_{sup}(\theta_{Student}) = -\frac{1}{N} \sum_{i=1}^N \left\{ \sum_{j=1}^k \{1\{y^{(i)} = j\} \times \log \left(\frac{e^{\theta_{Student_j}^T x^{(i)}}}{\sum_{l=1}^k e^{\theta_{Student_l}^T x^{(i)}}} \right) \} \right\} \quad (8)$$

The unsupervised loss is described by:

$$L_{unsup} = N_{Student}(I_t) - N_{Teacher}(I_{t_m}) \quad (9)$$

4. Experimental Results

We conducted experiments on three datasets for an image classification task:

1. **Office-31** dataset [43]. It consists of 31 categories and contains 4,110 images distributed over three domains: 1) **Amazon** domain which contains 2,817 images that are collected from Amazon.com, 2) **Webcam** domain containing 795 web camera images, and 3) **Dslr** domain containing 498 images from SLR cameras. In

our work we evaluate the transfer of $\mathbf{A} \rightarrow \{\mathbf{W}, \mathbf{D}\}$, $\mathbf{W} \rightarrow \{\mathbf{A}, \mathbf{D}\}$ and $\mathbf{D} \rightarrow \{\mathbf{W}, \mathbf{A}\}$.

2. **Office-Home** dataset [50]. It consists of 65 categories in 15,590 images over four domains: 1) **Art** domain with 2427 images, 2) **Clipart** domain of 4,365 images downloaded from multiple clipart websites, 3) **Product** domain of 4,439 images gathered from Amazon.com, and 4) **Real-world** domain of 4,357 images. **Art** and **Real-World** domains were built from websites like www.deviantart.com and www.flickr.com. In our work we evaluate the transfer task $\mathbf{Ar} \rightarrow \{\mathbf{Cl}, \mathbf{P}, \mathbf{R}\}$, $\mathbf{Cl} \rightarrow \{\mathbf{Ar}, \mathbf{P}, \mathbf{R}\}$, $\mathbf{P} \rightarrow \{\mathbf{Cl}, \mathbf{Ar}, \mathbf{R}\}$ and $\mathbf{R} \rightarrow \{\mathbf{Cl}, \mathbf{P}, \mathbf{Ar}\}$.

3. **Visual Domain Adaptation classification task (VisDa)** [38]. It consists of over 280K images across 12 categories across two domains: 1) **Synthetic** and 2) **Real**. In our work we evaluate the transfer between *Synthetic* \rightarrow *Real*.

CycleGAN-based Stochastic Style Transfer. The results of the Stochastic Style Transfer generation module are shown in Tables 1, 2, and 3, where Table 3 shows the results across multiple transfer tasks in all three datasets, while Tables 2 and 3 show results across different training epochs in the same transfer task across different training epochs. These results are shown in a Table format where each cell in the table contains two blocks of images. Each block consists of three rows, the first row represents the original images I_s or I_t for source and target domains respectively (source on the left, target on the right). The second row represents the output of applying the generator network to the input image denoted as I_{su} or I_{tu} for source and target images respectively. The third row represents the cycle reconstructed images I_{srec} or I_{trec} .

For training the module we used a batch size of 8, and we used the whole dataset in case of **Office-31**, but in the case of **Office-Home** we use 85% and in case of **VisDa** source we used 0.5% and 5% for the target. We did not sample the overall dataset in the cases of **Office-Home** and **VisDa** in order to reduce training time due to very small batch size in training. We choose $\lambda_i = 1$ in Eq 7 for $i = 1 \dots 6$

The results show that the module manages to create different image instances of the original domain that have style similar to the images of the other domain. Table 1 shows the transfer results for the Office-Home dataset between two domains $\mathbf{R} \rightarrow \mathbf{Ar}$ across different training epochs. It illustrates that the system managed to produce photo realistic results across many epochs except for epoch 25, where the results are little bit washed out. This demonstrates that with different statuses of the module parameters U_s and U_t we can obtain different style transfer results. The figures show that the module managed to keep the contents of the

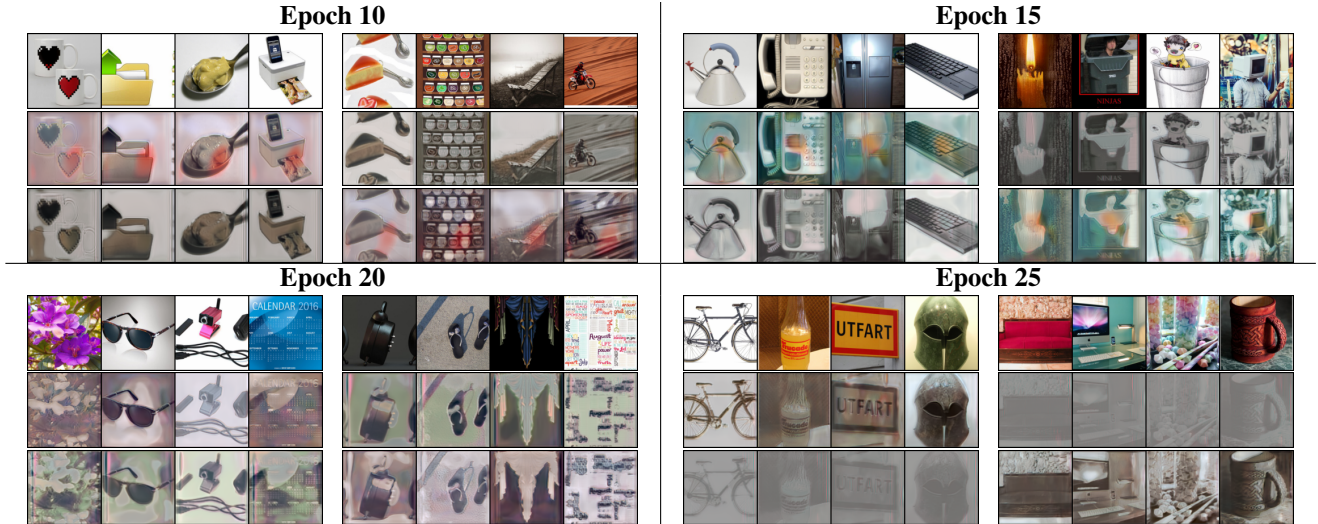


Table 1: The generation results for the $\mathbf{R} \longleftrightarrow \mathbf{Ar}$ transfer task in the **Office-Home** dataset across epochs 10, 15, 20, 25. Each quadrant represents results from one epoch, with the one on the left from \mathbf{R} domain while on the right is from the \mathbf{Ar} domain.

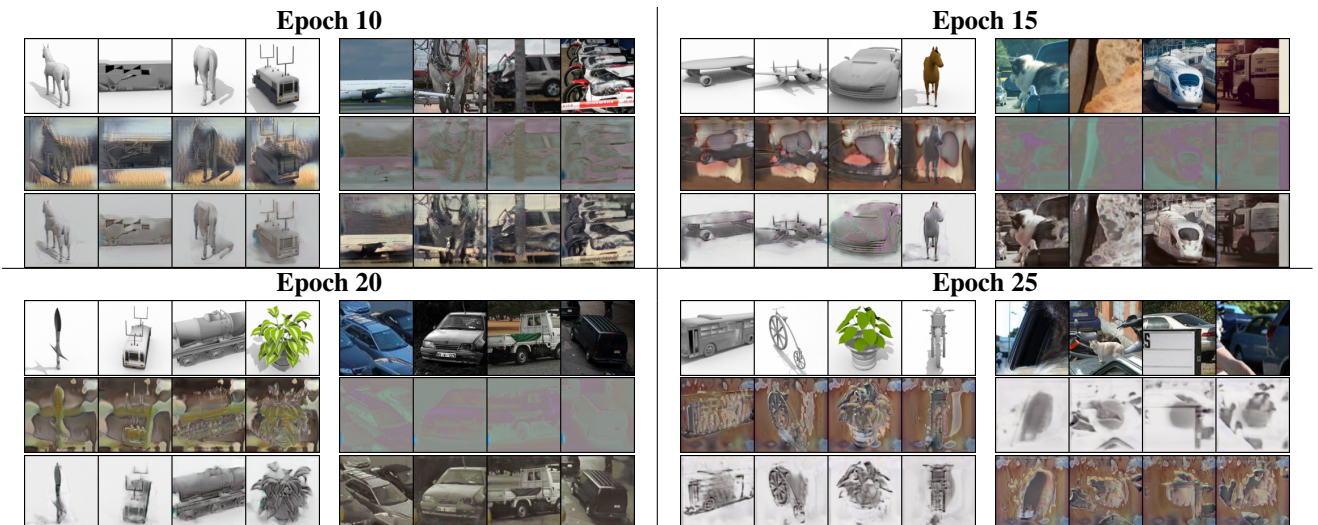


Table 2: The generation results for the $\mathbf{Sy} \longleftrightarrow \mathbf{Re}$ transfer task in the **VisDa** dataset across epochs 10, 15, 20, 25. In each quadrant, the left block of images represents the synthetic images while the right block represents the real images.

original domain but transfer the style of the other domain in a batch based mode. The results for the VisDa dataset are shown in Table 2. The performance is less compelling compared to the other dataset as it is a more challenging task. Still the system managed to produce good transfer results between the two domain as in Epoch 10 and Epoch 25. Finally results across all transfer tasks for all the datasets in Epoch 5 of the training algorithm are shown in Table 3. These results illustrate that the system managed to provide good results except for some cases as in **Office-Home** ($\mathbf{Art} \longleftrightarrow \mathbf{Product}$) and **VisDa** ($\mathbf{Synthetic} \longleftrightarrow \mathbf{Real}$).

For each domain's data we can generate many different instances of that data using the generation modules

trained for different transfer tasks. For example consider the **Amazon** domain in the **Office-31** dataset, which has its original version D_A and the version generated due to generation module ($\mathbf{Amazon} \longleftrightarrow \mathbf{Dslr}$) known as $D_{A,A,D}$ or due to the module ($\mathbf{Amazon} \longleftrightarrow \mathbf{Web}$) known as $D_{A,A,W}$. In each generation module we can choose training parameters stored from different training epochs (in our case we used epoch 5) and we can choose to get the images generated to be (I_{su}, I_{tu}) or the reconstructed images (I_{srec}, I_{trec}) (in our case we used (I_{su}, I_{tu})).

Self-ensemble zero shot domain adaptation. The classification results are shown in Tables 4b, 4a, and 4c for datasets **Office-31**, **Office-Home**, and **VisDa** datasets, re-

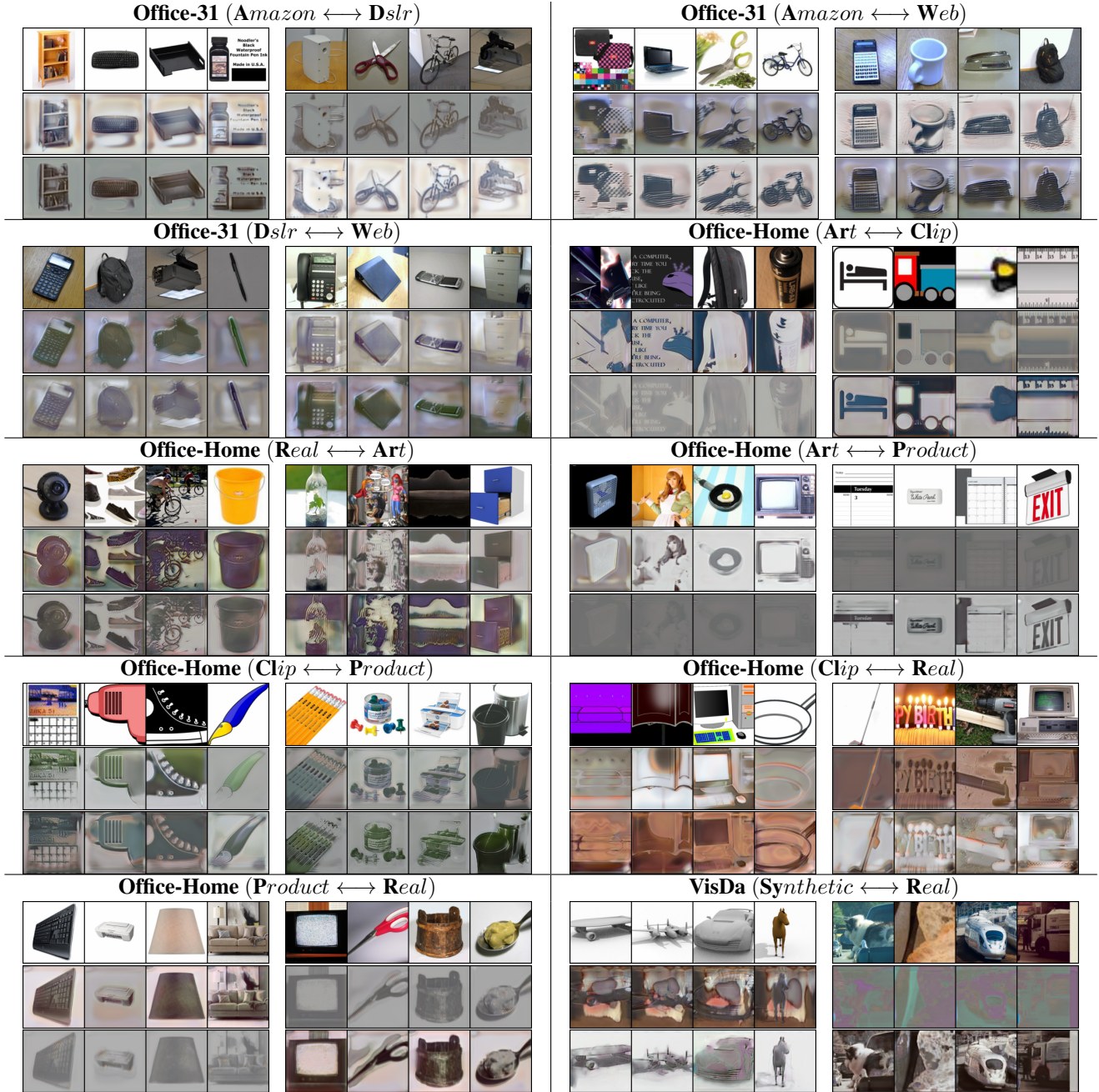


Table 3: The generation results of epoch 5 across the three datasets and the different transfer tasks. Each cell represents the result of one transfer task.

spectively. The color coding for both models and the datasets are shown in Table 4d. In our experiments we trained three different types of classification models with color codes in Table 4d: 1) Base model M_{base} : a model that has been trained on original source images only in a supervised way, the source datasets have color described by $Data_{T1}$ in Table 4d. 2) Tuned model M_{tune} : for a model that has been trained in a supervised way using the origi-

nal source images and the source mapped images (simple data augmentation to the source), the source datasets both have color described by $Data_{T1}$ in Table 4d. 3) M_{ensem} model: is a model trained in a supervised way using the data described by the source datasets (with color $Data_{T1}$) while trained in the unsupervised way using the target datasets with color described by $Data_{T3}$. Finally, all these models have been tested against other datasets that have not been in-

	M 0	M 1	M 2	M 3	M 4	M 5	M 6	M 7	M 8	M 9	M 10	M 11	M 12	M 13	M 14	M 15
D_{Ar}	0.8507	0.4898	0.4972	0.5985	0.7908	0.6044	0.8260	0.5127	0.5076	0.5193	0.8226	0.7608	0.8290	0.6745	0.6986	0.7200
$D_{Ar,Ar,Cl}$	0.3027	0.2065	0.1979	0.2312	0.5355	0.2550	0.3701	0.2527	0.2496	0.2204	0.5404	0.3530	0.4220	0.3211	0.3385	0.2954
$D_{Ar,Ar,R}$	0.5015	0.2784	0.2879	0.3288	0.5424	0.3920	0.6045	0.3381	0.3299	0.3284	0.5851	0.5390	0.6336	0.4667	0.4715	0.4876
$D_{Ar,Ar,P}$	0.4693	0.2765	0.2907	0.3374	0.5186	0.4093	0.6589	0.3434	0.3380	0.3228	0.5819	0.5186	0.6496	0.4445	0.4575	0.4477
D_{Cl}	0.5092	0.8009	0.4856	0.5320	0.4706	0.5023	0.4919	0.7924	0.7905	0.4790	0.5490	0.5511	0.5376	0.7410	0.7036	0.5337
$D_{Cl,Cl,Ar}$	0.3306	0.4695	0.2895	0.3262	0.3770	0.3542	0.3698	0.5546	0.5896	0.3308	0.4143	0.4224	0.4029	0.6010	0.5933	0.3798
$D_{Cl,Cl,P}$	0.3259	0.4427	0.2967	0.3264	0.3816	0.3718	0.3907	0.6592	0.5674	0.3349	0.4195	0.4394	0.4206	0.6740	0.5810	0.3929
$D_{Cl,Cl,R}$	0.3469	0.4836	0.3139	0.3328	0.3967	0.3771	0.3914	0.5685	0.6659	0.3382	0.4175	0.4405	0.3953	0.5988	0.6269	0.3812
D_P	0.6261	0.5785	0.9074	0.7276	0.5815	0.7103	0.6227	0.6012	0.6128	0.9090	0.6493	0.7017	0.6589	0.6383	0.6335	0.8370
$D_{P,Ar,P}$	0.3173	0.2529	0.4147	0.3112	0.3110	0.3587	0.3501	0.3522	0.3106	0.4667	0.3450	0.4322	0.3768	0.4043	0.3964	0.5538
$D_{P,Cl,P}$	0.4256	0.3695	0.5605	0.4486	0.4218	0.5035	0.4424	0.4291	0.4238	0.6832	0.4633	0.5534	0.4965	0.4980	0.4945	0.7168
$D_{P,P,R}$	0.4885	0.4229	0.6851	0.5363	0.4638	0.5785	0.5029	0.4745	0.4885	0.8371	0.5223	0.6164	0.5414	0.5413	0.5403	0.7950
D_R	0.7113	0.6296	0.6998	0.8964	0.6688	0.8737	0.7020	0.6472	0.6403	0.7188	0.6975	0.7786	0.7205	0.6830	0.6806	0.7537
$D_{R,Ar,R}$	0.4773	0.3766	0.4036	0.5354	0.4847	0.7461	0.5348	0.4476	0.4399	0.4606	0.5084	0.6700	0.5436	0.5221	0.5310	0.5326
$D_{R,Cl,R}$	0.2900	0.2769	0.2821	0.3278	0.3584	0.3876	0.3398	0.3168	0.3197	0.3013	0.3861	0.4339	0.3550	0.3853	0.3987	0.3473
$D_{R,P,R}$	0.5084	0.4024	0.4574	0.6071	0.4970	0.6863	0.5355	0.4745	0.4638	0.5079	0.5363	0.6458	0.5647	0.5442	0.5480	0.5885

(a) Top-5 classification results for **Office-Home** dataset, showing that model **M 11** achieves the best performance across all other transfer tasks.

	M 0	M 1	M 2	M 3	M 4	M 5	M 6	M 7	M 8
D_A	0.904	0.006	0.0038	0.901	0.885	0.622	0.959	0.955	0.868
$D_{A,A,D}$	0.551	0.012	0.0012	0.806	0.742	0.548	0.866	0.823	0.700
$D_{A,A,W}$	0.578	0.029	0.00	0.721	0.790	0.545	0.834	0.857	0.690
D_D	0.728	0.650	0.549	0.775	0.795	0.973	0.855	0.865	0.994
$D_{D,A,D}$	0.482	0.136	0.156	0.587	0.631	0.853	0.690	0.696	0.901
$D_{D,W,D}$	0.418	0.091	0.169	0.524	0.592	0.899	0.634	0.673	0.968
D_W	0.692	0.34	0.553	0.750	0.754	0.934	0.832	0.838	0.979
$D_{W,W,A}$	0.429	0.040	0.056	0.517	0.560	0.801	0.600	0.624	0.823
$D_{W,W,D}$	0.472	0.068	0.139	0.591	0.601	0.858	0.677	0.691	0.918

(b) Top-5 classification results for **Office-31** dataset, showing that model **M 8** achieves the best performance across all other transfer tasks.

involved in training, either supervised or unsupervised, with color described by $Data_{T4}$.

Results Analysis. The performance results show that there is a model that has the highest performance on all other target domains. Table 4b presents the results of the **Office-31** dataset showing that Model M 8 has the highest performance across all the other transfer tasks. This model has been trained using the proposed method with supervised source data D_D and $D_{D,W,D}$ while trained on D_W and $D_{W,W,D}$ in an unsupervised way. Despite that this model has never seen any instance of domain A , it has the highest transfer performance across all instances of domain A . Similarly, the results of the **Office-Home** dataset are shown in Table 4a. From this table, we can see that model M 11 has the highest performance over all other target datasets except one case of data D_P . This model was trained on D_R and $D_{R,Ar,R}$ in a supervised way while it was trained on D_{Ar} and $D_{Ar,Ar,R}$ in an unsupervised way, and managed to generalize across other domains of P, Cl without seeing these data. These results are consistent with Top-1 results. Finally, the results of **VisDA** are presented in Table 4c, showing that model M 1 achieves the best transfer top-5 results, while on top-1, M 2 and M 3 achieve best results on D_{Re} and $D_{Re,Re,Sy}$ respectively. No single model managed to get

M_{base}	$Data_{T1}$
M_{tune}	$Data_{T2}$
M_{ensemb}	$Data_{T3}$
	$Data_{T4}$

(d) Color coding of the results for both models and datasets.

	M 0	M 1	M 2	M 3
D_{Sy}	0.954 (0.799)	0.934 (0.789)	0.909 (0.777)	0.916 (0.786)
$D_{Sy,Sy,Re}$	0.753 (0.270)	0.948 (0.747)	0.889 (0.746)	0.892 (0.742)
D_{Re}	0.605 (0.183)	0.731 (0.387)	0.700 (0.395)	0.705 (0.394)
$D_{Re,Re,Sy}$	0.511 (0.142)	0.577 (0.192)	0.553 (0.194)	0.559 (0.195)

(c) Top-5 (Top-1) Classification performance results for **VisDa**.

higher performance, we believe this is due to less quality of Generated random instances shown in Table 2

5. Conclusion and Future Work

In this work, we showed that domain adaptation can benefit from generative models to enhance network generalization performance across multiple other domains. We demonstrated that these networks can produce multiple random instances of the same domain dataset. Each instance represents a random different shift compared to the original dataset. Our results also show that using a self-ensemble method is better than simple data augmentation to enhance knowledge transfer performance even on unseen domains. In the future we plan to train the model end-to-end where each epoch of the generation module produces data with new random domain shifts and train the classifier incrementally, so that the model can generalize across continuous domain shift changes. Moreover, we plan to conduct experiments in which we compare the highest performing model across different methods in different transfer tasks in the same dataset, which we did not do here because our goal was to show that a model can generalize even across unseen domains by using the generative models, which to our knowledge has not been done before.

References

- [1] R. Aljundi, R. Emonet, D. Muselet, and M. Sebban. Landmarks-based kernelized subspace alignment for unsupervised domain adaptation. In *Proceedings of the IEEE Conference on Computer Vision and Pattern Recognition*, pages 56–63, 2015. 2
- [2] P. Bachman, O. Alsharif, and D. Precup. Learning with pseudo-ensembles. In *Advances in Neural Information Processing Systems*, pages 3365–3373, 2014. 4
- [3] M. Baktashmotlagh, M. T. Harandi, B. C. Lovell, and M. Salzmann. Domain adaptation on the statistical manifold. In *Proceedings of the IEEE Conference on Computer Vision and Pattern Recognition*, pages 2481–2488, 2014. 2
- [4] K. Bousmalis, N. Silberman, D. Dohan, D. Erhan, and D. Krishnan. Unsupervised pixel-level domain adaptation with generative adversarial networks. In *The IEEE Conference on Computer Vision and Pattern Recognition (CVPR)*, volume 1, page 7, 2017. 1, 2
- [5] K. Bousmalis, G. Trigeorgis, N. Silberman, D. Krishnan, and D. Erhan. Domain separation networks. In *Advances in Neural Information Processing Systems*, pages 343–351, 2016. 1, 2
- [6] G. Csurka. Domain adaptation for visual applications: A comprehensive survey. *arXiv preprint arXiv:1702.05374*, 2017. 2
- [7] J. V. Davis, B. Kulis, P. Jain, S. Sra, and I. S. Dhillon. Information-theoretic metric learning. In *Proceedings of the 24th international conference on Machine learning*, pages 209–216. ACM, 2007. 2
- [8] G. French, M. Mackiewicz, and M. Fisher. Self-ensembling for visual domain adaptation. In *ICLR*, 2018. 1, 3, 5
- [9] Y. Ganin, E. Ustinova, H. Ajakan, P. Germain, H. Larochelle, F. Laviolette, M. Marchand, and V. Lempitsky. Domain-adversarial training of neural networks. *The Journal of Machine Learning Research*, 17(1):2096–2030, 2016. 2
- [10] Y. Ganin, E. Ustinova, H. Ajakan, P. Germain, H. Larochelle, F. Laviolette, M. Marchand, and V. Lempitsky. Domain-adversarial training of neural networks. *The Journal of Machine Learning Research*, 17(1):2096–2030, 2016. 2
- [11] L. Gatys, A. Ecker, and M. Bethge. A neural algorithm of artistic style. *Nature Communications*, 2015. 3
- [12] W. Ge and Y. Yu. Borrowing treasures from the wealthy: Deep transfer learning through selective joint fine-tuning. *Advances in neural information processing systems*, 19(41):2, 2007. 2
- [13] M. Ghifary, W. Bastiaan Kleijn, M. Zhang, and D. Balduzzi. Domain generalization for object recognition with multi-task autoencoders. In *Proceedings of the IEEE international conference on computer vision*, pages 2551–2559, 2015. 2
- [14] M. Ghifary, W. B. Kleijn, M. Zhang, D. Balduzzi, and W. Li. Deep reconstruction-classification networks for unsupervised domain adaptation. In *European Conference on Computer Vision*, pages 597–613. Springer, 2016. 2
- [15] B. Gong, K. Grauman, and F. Sha. Connecting the dots with landmarks: Discriminatively learning domain-invariant features for unsupervised domain adaptation. In *International Conference on Machine Learning*, pages 222–230, 2013. 2
- [16] I. Goodfellow, J. Pouget-Abadie, M. Mirza, B. Xu, D. Warde-Farley, S. Ozair, A. Courville, and Y. Bengio. Generative adversarial nets. In *Advances in neural information processing systems*, pages 2672–2680, 2014. 1
- [17] G. Hinton, O. Vinyals, and J. Dean. Distilling the knowledge in a neural network. *stat*, 1050:9, 2015. 2
- [18] E. Hosseini-Asl, Y. Zhou, C. Xiong, and R. Socher. Augmented cyclic adversarial learning for domain adaptation. *arXiv preprint arXiv:1807.00374*, 2018. 1, 3
- [19] J. Huang, A. Gretton, K. M. Borgwardt, B. Schölkopf, and A. J. Smola. Correcting sample selection bias by unlabeled data. In *Advances in neural information processing systems*, pages 601–608, 2007. 2
- [20] X. Huang, Y. Li, O. Poursaeed, J. Hopcroft, and S. Belongie. Stacked generative adversarial networks. In *2017 IEEE Conference on Computer Vision and Pattern Recognition (CVPR)*, pages 1866–1875. IEEE, 2017. 1
- [21] P. Isola, J.-Y. Zhu, T. Zhou, and A. A. Efros. Image-to-image translation with conditional adversarial networks. In *2017 IEEE Conference on Computer Vision and Pattern Recognition (CVPR)*, pages 5967–5976. IEEE, 2017. 3
- [22] G. Kang, L. Zheng, Y. Yan, and Y. Yang. Deep adversarial attention alignment for unsupervised domain adaptation: the benefit of target expectation maximization. *arXiv preprint arXiv:1801.10068*, 2018. 1, 3
- [23] T. Karras, T. Aila, S. Laine, and J. Lehtinen. Progressive growing of gans for improved quality, stability, and variation. In *ICLR*, 2018. 1
- [24] A. Krizhevsky, I. Sutskever, and G. E. Hinton. Imagenet classification with deep convolutional neural networks. In *Advances in neural information processing systems*, pages 1097–1105, 2012. 1
- [25] B. Kulis, K. Saenko, and T. Darrell. What you saw is not what you get: Domain adaptation using asymmetric kernel transforms. In *Computer Vision and Pattern Recognition (CVPR), 2011 IEEE Conference on*, pages 1785–1792. IEEE, 2011. 2
- [26] S. Laine and T. Aila. Temporal ensembling for semi-supervised learning. In *ICLR*, 2017. 3
- [27] C. Ledig, L. Theis, F. Huszar, J. Caballero, A. Cunningham, A. Acosta, A. Aitken, A. Tejani, J. Totz, Z. Wang, et al. Photo-realistic single image super-resolution using a generative adversarial network. In *Proceedings of the IEEE Conference on Computer Vision and Pattern Recognition*, pages 4681–4690, 2017. 1
- [28] M.-Y. Liu, T. Breuel, and J. Kautz. Unsupervised image-to-image translation networks. In *Advances in Neural Information Processing Systems*, pages 700–708, 2017. 3
- [29] M.-Y. Liu and O. Tuzel. Coupled generative adversarial networks. In *Advances in neural information processing systems*, pages 469–477, 2016. 2
- [30] J. Long, E. Shelhamer, and T. Darrell. Fully convolutional networks for semantic segmentation. In *The IEEE Conference on Computer Vision and Pattern Recognition (CVPR)*, June 2015. 1
- [31] M. Long, Y. Cao, J. Wang, and M. I. Jordan. Learning transferable features with deep adaptation networks. In *Pro-*

- ceedings of the 32nd International Conference on Machine Learning (ICML)*, 2015. 2
- [32] M. Long, H. Zhu, J. Wang, and M. I. Jordan. Deep transfer learning with joint adaptation networks. In *Proceedings of the 34th International Conference on Machine Learning (ICML)*, 2017. 2
- [33] Y. Luo, J. Zhu, M. Li, Y. Ren, and B. Zhang. Smooth neighbors on teacher graphs for semi-supervised learning. In *IEEE International Conference on Computer Vision*, 2018. 3
- [34] T. Miyato, S.-i. Maeda, S. Ishii, and M. Koyama. Virtual adversarial training: a regularization method for supervised and semi-supervised learning. *IEEE transactions on pattern analysis and machine intelligence*, 2018. 4
- [35] Z. Murez, S. Kolouri, D. Kriegman, R. Ramamoorthi, and K. Kim. Image to image translation for domain adaptation. In *IEEE International Conference on Computer Vision*, 2017. 3
- [36] D. Pathak, P. Krahenbuhl, J. Donahue, T. Darrell, and A. A. Efros. Context encoders: Feature learning by inpainting. In *Proceedings of the IEEE Conference on Computer Vision and Pattern Recognition*, pages 2536–2544, 2016. 1
- [37] X. Peng and K. Saenko. Synthetic to real adaptation with generative correlation alignment networks. In *2018 IEEE Winter Conference on Applications of Computer Vision (WACV)*, pages 1982–1991. IEEE, 2018. 3
- [38] X. Peng, B. Usman, N. Kaushik, J. Hoffman, D. Wang, and K. Saenko. Visda: The visual domain adaptation challenge. *arXiv preprint arXiv:1710.06924*, 2017. 2, 5
- [39] A. Radford, L. Metz, and S. Chintala. Unsupervised representation learning with deep convolutional generative adversarial networks. In *ICLR*, 2015. 1
- [40] A. Rasmus, M. Berglund, M. Honkala, H. Valpola, and T. Raiko. Semi-supervised learning with ladder networks. In *Advances in Neural Information Processing Systems*, pages 3546–3554, 2015. 4
- [41] S. Ren, K. He, R. Girshick, and J. Sun. Faster r-cnn: Towards real-time object detection with region proposal networks. In *Advances in neural information processing systems*, pages 91–99, 2015. 1
- [42] O. Ronneberger, P. Fischer, and T. Brox. U-net: Convolutional networks for biomedical image segmentation. In *International Conference on Medical image computing and computer-assisted intervention*, pages 234–241. Springer, 2015. 3
- [43] K. Saenko, B. Kulis, M. Fritz, and T. Darrell. Adapting visual category models to new domains. In *European conference on computer vision*, pages 213–226. Springer, 2010. 2, 4, 5
- [44] K. Simonyan and A. Zisserman. Very deep convolutional networks for large-scale image recognition. In *Proc. International Conference on Learning Representations*, 2015. 3
- [45] B. Sun, J. Feng, and K. Saenko. Return of frustratingly easy domain adaptation. In *Thirtieth AAAI Conference on Artificial Intelligence*, 2016. 2
- [46] B. Sun and K. Saenko. Deep coral: Correlation alignment for deep domain adaptation. In *European Conference on Computer Vision*, pages 443–450. Springer, 2016. 2
- [47] A. Tarvainen and H. Valpola. Mean teachers are better role models: Weight-averaged consistency targets improve semi-supervised deep learning results. In *Advances in neural information processing systems*, pages 1195–1204, 2017. 3
- [48] E. Tzeng, J. Hoffman, T. Darrell, and K. Saenko. Simultaneous deep transfer across domains and tasks. In *Proceedings of the IEEE International Conference on Computer Vision*, pages 4068–4076, 2015. 2
- [49] E. Tzeng, J. Hoffman, K. Saenko, and T. Darrell. Adversarial discriminative domain adaptation. In *2017 IEEE Conference on Computer Vision and Pattern Recognition (CVPR)*, pages 2962–2971. IEEE, 2017. 2
- [50] H. Venkateswara, J. Eusebio, S. Chakraborty, and S. Panchanathan. Deep hashing network for unsupervised domain adaptation. In *Computer Vision and Pattern Recognition (CVPR), 2017 IEEE Conference on*, pages 5385–5394. IEEE, 2017. 2, 5
- [51] H. Yan, Y. Ding, P. Li, Q. Wang, Y. Xu, and W. Zuo. Mind the class weight bias: Weighted maximum mean discrepancy for unsupervised domain adaptation. In *Computer Vision and Pattern Recognition (CVPR), 2017 IEEE Conference on*, pages 945–954. IEEE, 2017. 2
- [52] S. Zagoruyko and N. Komodakis. Paying more attention to attention: Improving the performance of convolutional neural networks via attention transfer. In *ICLR*, 2017. 3
- [53] Z.-J. Zha, T. Mei, M. Wang, Z. Wang, and X.-S. Hua. Robust distance metric learning with auxiliary knowledge. In *IJCAI*, pages 1327–1332, 2009. 2
- [54] J.-Y. Zhu, T. Park, P. Isola, and A. A. Efros. Unpaired image-to-image translation using cycle-consistent adversarial networks. In *IEEE International Conference on Computer Vision*, 2017. 1, 3
- [55] J.-Y. Zhu, R. Zhang, D. Pathak, T. Darrell, A. A. Efros, O. Wang, and E. Shechtman. Toward multimodal image-to-image translation. In *Advances in Neural Information Processing Systems*, pages 465–476, 2017. 3